Interdisciplinary CardioVascular and Thoracic Surgery 2025, 40(11), ivaf265
https://doi.org/10.1093/icvts/ivaf265 Advance Access publication 6 November 2025

ORIGINAL ARTICLE

Cite this article as: Catalano C, Pasta S, Potratz P, Buffle E, Siepe M, Obrist D. Haemodynamic Performance of Transcatheter Heart Valve in Bileaflet Mechanical Valve: An *In-vitro* Study. Interdiscip CardioVasc Thorac Surg 2025; doi:10.1093/icvts/ivaf265.

VALVULAR HEART DISEASE

# Haemodynamic Performance of Transcatheter Heart Valve in Bileaflet Mechanical Valve: An *In-vitro* Study

**Chiara Catalano**[*,1,2]; **Salvatore Pasta**[1,2]; **Paul Potratz**[3]; **Eric Buffle**[4]; **Matthias Siepe**[3]; **Dominik Obrist**[5]

[1]Department of Engineering, Viale delle Scienze, Università degli Studi di Palermo, Palermo, 90128, Italy
[2]Department of Research, IRCCS ISMETT via Tricomi, Palermo, 90127, Italy
[3]Department of Cardiac Surgery, Inselspital, Bern University Hospital, and University of Bern, Bern, 3010, Switzerland
[4]Department of Cardiology, Inselspital, Bern University Hospital, and University of Bern, Bern, 3010, Switzerland
[5]ARTORG Center for Biomedical Engineering Research, University of Bern, Bern, 3008, Switzerland

*Corresponding author. Department of Engineering, Università degli Studi di Palermo, Viale delle Scienze, Ed. 8, 90128, Palermo, Italy (chiara.catalano02@unipa.it).

Received: August 13, 2025; Revised: October 2, 2025; Accepted: October 20, 2025

## Graphical abstract

**The Hemodynamic Performance of a Transcatheter Heart Valve In a Bileaflet Mechanical Valve (Valve-in-MHV): An In-Vitro Study**

**Summary**

Backlight PIV and a left heart mock loop were used to assess the hemodynamics of a novel hybrid configuration, involving the surgical implantation of the CoreValve THV within a SJM composite valved graft after removal of the leaflets. The resulting valve-in-MHV exhibited a more physiological flow pattern compared to the MHV alone, though high velocities and turbulence were observed.

**Comparison of Valve Performance Metrics**

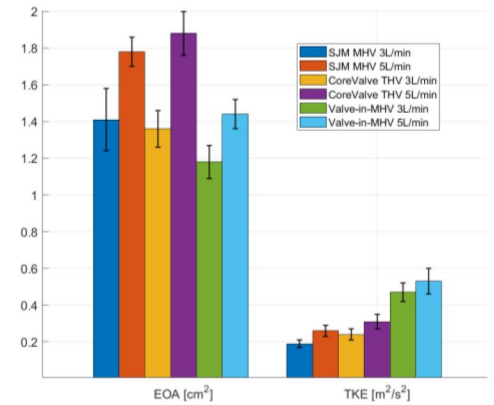


Legend: PIV – Particle Image Velocimetry; THV – Transcatheter Hear Valve; SJM – St. Jude Medical; MHV – Mechanical Heart Valve; EOA – Effective Orifice Area; TKE – Turbulent Kinetic Energy.

## Abstract

**Objectives:** This study evaluates the haemodynamic performance of a novel hybrid configuration—Valve-in-MHV—where a CoreValve transcatheter heart valve is implanted within the annulus of a composite valved graft after leaflet removal.

**Methods:** *In vitro* testing was performed using left heart mock loop combined with backlight particle image velocimetry. Three configurations were assessed: (i) mechanical heart valve (MHV), (ii) CoreValve THV, and (iii) Valve-in-MHV. Flow parameters were measured at cardiac outputs of 3 and 5 L/min.

**Results:** At 5 L/min, the Valve-in-MHV showed the highest PG (15.5 mmHg) and TKE (0.53 $m^2/s^2$), compared to the THV (10.9 mmHg, 0.31 $m^2/s^2$) and MHV (11.5 mmHg, 0.26 $m^2/s^2$). Effective orifice area was smallest for the Valve-in-MHV (1.44 $cm^2$). The Valve-in-MHV generated a more physiological central jet than the MHV, but with increased turbulence and higher peak velocities (up to 2.66 m/s).

**Conclusions:** Examining the mechanistic implications of Valve-in-MHV may offer valuable insights into the likelihood of adverse effects such as leaflet thrombosis and the development of pronounced pressure gradients in patients who are candidates for Valve-in-MHV.

**Keywords:** bioprosthesis; particle image velocimetry; surgical aortic valve replacement.

## INTRODUCTION

Aortic valve replacement, through surgical or transcatheter approaches, has revolutionized the management of valvular diseases.[1] Mechanical heart valves (MHVs) and biological heart valves (BHVs) represent the 2 main choices for valve replacement, but they both carry inherent limitations.[2] Biological valves, as transcatheter heart valves (THVs) or surgical bioprostheses, are preferred for providing physiological flow. However, they are constrained by a limited lifespan, often necessitating reoperation due to structural valve degeneration (SVD).[3] Conversely, MHVs, which are frequently used in combination with synthetic vascular grafts (ie, composite valved graft)[4] for aortic root replacement and coronary ostial reimplantation, are known for their long-term durability. Nonetheless, they are associated with a high risk of thromboembolic events, requiring lifelong anticoagulation therapy and exposing patients to significant bleeding risks.[5] In addition, some patients cannot hold out the gentle click sound associated to a variable degree with MHVs. These trade-offs highlight the need for innovative approaches that balance device durability and thrombogenic risk in case of MHV failure. In the event of prosthetic valve dysfunction, patients with composite valved graft typically face high-risk reoperation involving complete explantation of the graft and valve. This procedure is technically demanding and associated with significant surgical risk. A less invasive alternative could involve removing the leaflets while retaining the annular ring of the valve, thereby allowing the THV implantation directly into the remaining ring. This technique may simplify reintervention while preserving annular stability and could reduce leaflet-related sources of thrombogenicity.

In this context, experimental flow investigations could effectively enhance the understanding on device performance.[6–8] However, research has largely focused on the investigation of individual valve types, with limited attention given to studies involving the integration of multiple devices.

The motivation for this study arises from a specific clinical scenario: a patient with cerebral bleeding caused by anticoagulation therapy required for an implanted composite valved graft, incorporating the St Jude Medical (SJM) MHV in a woven Dacron Valsalva graft.[9] Complete exchange to biological valved conduit is a far bigger operation than MHV's leaflet removal and implantation of a TAVI prosthesis in the mechanical cage. To explore this, *in vitro* experiments utilizing backlight particle image velocimetry (PIV) were conducted in a cardiac flow loop to evaluate the fluid dynamics of the hybrid configuration, referred to as valve-in-MHV. Specifically, this novel configuration involved the removal of the composite valved graft's leaflets, followed by the implantation of the Medtronic CoreValve THV within its annulus. The resulting configuration was compared to standalone MHV and THV to elucidate haemodynamic factors that may influence clinical outcomes when implementing the proposed hybrid configuration in cardiac surgery. This study aims to determine if the proposed hybrid approach can address the limitations of conventional valve replacements, providing a viable bailout option in cases where reoperation carries prohibitive risk. By exploring the haemodynamic performance of such configuration, this work contributes to developing innovative strategies that optimize valve replacement and expand treatment options for complex cases.

## METHODS

*In vitro* haemodynamic assessment of 3 aortic valve configurations was performed using backlight PIV and a pulse duplicator system resembling the cardiac left heart circulation. The objective of the study was to quantify the flow performance of the CoreValve THV when implanted in the annulus of a SJM MHV with its mechanical leaflets removed. The haemodynamic performance of this procedure, referred to as valve-in-MHV, was compared to that of a single MHV and THV to elucidate the haemodynamic factors that may influence clinical outcomes when implementing the proposed configuration in cardiac surgery.

### Pulse duplicator system

The experimental pulse duplicator system (**Figure 1A**) consisted of a hydraulic flow loop equipped with a pulsatile piston pump, a ventricular chamber, the test, a compliance chamber, the resistance element, a fluid reservoir, and flow and pressure transducers. The piston pump (ViVitro Inc., Victoria, BC, Canada) allowed to generate physiological pulsatile flow by means of a piston compressing blood mimicking fluid (BMF) with a silicone membrane interface in the left ventricle chamber. The silicone membrane acts as a contracting left ventricle, generating pulsatile flow through the test cell where the aortic valve is located. Then, the flow passes through the compliance chamber and is finally recirculated to the left atrium chamber via a resistance element modelling the systemic resistance. The left ventricle and left atrium chambers were connected via a bi-leaflet mechanical device representing the mitral valve. The position of the piston was tracked using a linear variable differential transformer (LVDT) sensor mounted on the piston. Two pressure transducers (PX600F 150B, Edwards Lifesciences, CA, USA) were placed in the ventricle and compliance chambers to measure the ventricle and aortic pressures, respectively, and to derive the transvalvular pressure gradient (PG). Additionally, an ultrasonic flow probe (TS410/ME-11PXL, Transonic Systems, Inc., Ithaca, NY) was positioned downstream of the compliance chamber to measure the cardiac output (CO). Further details of the set-up can be found in previously published work of our group.[10]

The test section of the pulse duplicator comprised a thick-walled-silicon model to house the valves. The model was fabricated using transparent silicone (Sylgard 184, The Dow Chemical Company, Midland, MI, USA) with a refractive index (RI) of 1.410.

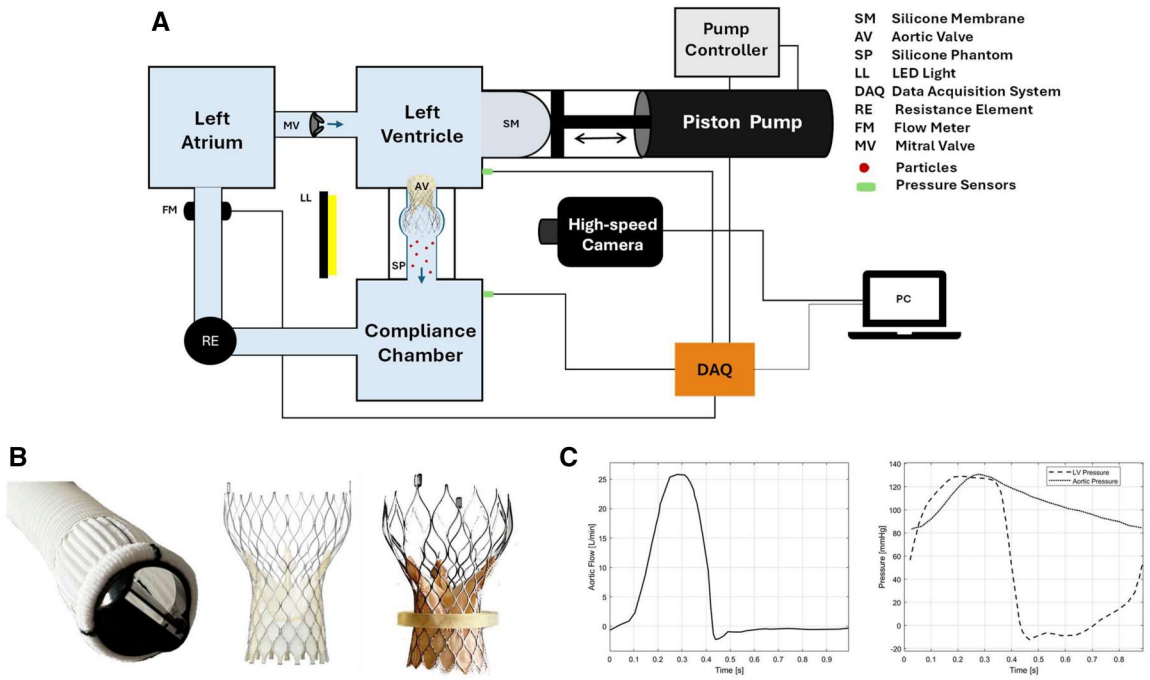


**Figure 1.** (A) Pulse duplicator and PIV system set-up. (B) Tested valves (from left: SJM MHV, THV, valve-in-MHV). (C) Representative physiological conditions

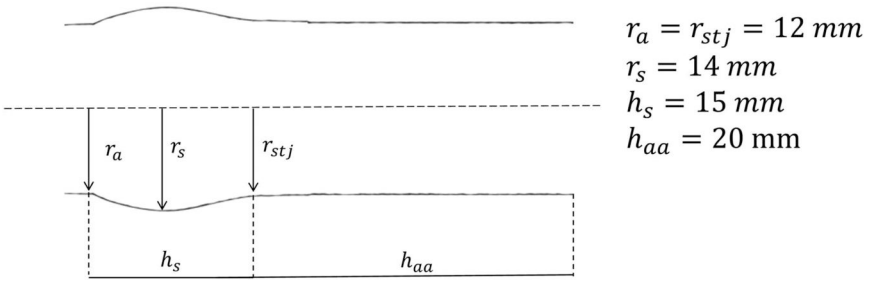


**Figure 2.** Geometry and Measurements of the Silicone Phantom Resembling the Valsava Dacron Graft

The mould for casting the silicone was designed to resemble a Dacron graft[11] (**Figure 2**) using the CAD software Rhinoceros (McNeel & Associates, USA) and subsequently 3D-printed with stiff resin material.

The selection of a thick-walled model was justified by the circumferential stiffness of the graft, ensuring the absence of significant circumferential deformations.[12] Additionally, a stiff resin ring was 3D-printed to model the SJM MHV annulus ring, eliminating the need to remove the leaflets from the real MHV. The CAD (Computer Aided Design) model was obtained by acquiring the SJM valve using high-resolution micro-CT scanner.

For the BMF, a mix of water, glycerol, and sodium chloride (wt% 49.4, 34, 16.6) was utilized. This mixture was shown to have rheological properties similar to that of blood (at 22°C, density $\rho = 1200\ kg/m^3$, dynamic viscosity $\mu = 5.6$ mPa s), while also matching the RI of the silicone to minimize distortion during image acquisitions.[13]

## PIV system

The overall PIV system integrated with the pulse duplicator is shown in **Figure 1A**. PIV analysis was implemented to measure flow velocities and estimate turbulence dissipation. This technique involved using a high-speed camera and a LED backlight to illuminate particles dispersed in the fluid volume within the aortic root model.

The BMF was seeded with fluorescent red microspheres provided by Cospheric LLC (density $\rho = 1200\ kg/m^3$), composed of polyethylene with diameters ranging from 355 to 425 μm. The seeding density was estimated to be approximately 5 g of particles dispersed in 8 L of BMF, resulting in an effective Stokes number of 0.069. A high-speed camera (Photron FASTCAM Mini AX 100) fitted with a Samyang fixed-focus lens featuring a 100 mm focal length and an aperture of f/2.8 was used to capture lateral images of the tested valves. A frame rate of 2500 fps was selected, with a window size of 1024 × 1024 pixels. The pixel size was 67.95 μm and time-resolved PIV images were captured using an external trigger provided by the pump controller. The software PIVlab 3.01 (Matlab v2022, Mathworks, USA) was used for camera calibration, images pre-processing and PIV analysis.[14] Velocity vectors were computed from spatial time-series cross-correlation of the images within an interrogation window of 128 × 128 pixels with a 50% overlap. This was followed by an interrogation pass with smaller window sizes of 64 × 64 and 32 × 32 pixels to enhance the signal of the correlation peak.

## Experimental protocol

A total of 6 experiments were conducted by examining and analysing 3 valve configurations under 2 distinct physiological conditions: (i) 21-mm SJM bi-leaflet mechanical heart valve (ie, SJM MHV) housed within a 24-mm Dacron graft, (ii) 26-mm Medtronic CoreValve (ie, CoreValve THV), and (iii) hybrid configuration with the THV in the 3D-printed model of the SJM MHV valve ring (ie, the Valve-in-MHV) (**Figure 1B**). Each configuration was tested under 2 different haemodynamic configurations: (i) 72 bpm with aortic pressure of 120/80 mmHg and CO of 5.0 L/min; and (ii) 72 bpm with aortic pressure of 100/60 and CO of 3 L/min. All measurements were captured at a frequency of 1000 Hz using a NI 6221 data acquisition (DAQ) device (National Instruments), employing an in-house developed Matlab script. Systolic performance of the valve configuration was evaluated based on the effective orifice area (EOA), calculated using Gorlin's equation[15]:

$$EOA = \frac{Q_{RMS}}{51.6\sqrt{PG}} \ (cm^2)$$

where $Q_{RMS}\left(\frac{ml}{s}\right)$ represents the root mean square value of aortic flow during forward flow.

Instantaneous flow fields were calculated over $N = 30$ heartbeats at specific phases $\phi$ of the cardiac cycle, whose duration is denoted by T. With $n = 1, 2, \ldots, N$, each acquisition took place at time $t = t_\phi + (n-1)T$. As outlined by Ferrari et al,[16] mean velocities were determined by phase-averaging the instantaneous velocity fields and were expressed as follows:

$$\overline{v}_x(t_\phi) = \frac{1}{N}\sum_{n=1}^{N} v_x(t_\phi + (n-1)T)$$

The cardiac cycle phases were defined with systole represented as the first 35% of the cycle duration and were specified as follows: early systole occurring at $t_\phi = 0.05$, peak systole occurring at $t_\phi = 0.15$, and diastole beginning at $t_\phi = 0.35$.

## Flow field analysis

According to the Reynolds decomposition, the velocity field $\boldsymbol{v}$ can be represented as the sum of the mean velocity field $\overline{\boldsymbol{v}}$ and the velocity fluctuations $\boldsymbol{v}'$ around the mean[17]:

$$\boldsymbol{v} = \overline{\boldsymbol{v}} + \boldsymbol{v}'$$

The root mean square of the velocity fluctuations was measured as:

$$v'_{rms} = \sqrt{\overline{v_x'^2} + \overline{v_y'^2}}$$

Therefore, the turbulent kinetic energy (TKE, $m^2/s^2$) and Reynolds shear stress (RSS, Pa), associated with turbulence levels and platelet activation,[18,19] were defined as follows:

$$TKE = \frac{1}{2}\left(\overline{v_x'^2} + \overline{v_y'^2}\right)$$

$$RSS = \rho\sqrt{\left(\frac{\overline{v_x'^2} - \overline{v_y'^2}}{2}\right)^2 + \left(\overline{v_x' v_y'}\right)^2}$$

where $v_x'$ and $v_y'$ are the instantaneous velocity fluctuations in the x and y direction, respectively, and $\rho$ is the blood density. Statistical analysis was performed using SigmaPlot 14.0. The one-way ANOVA test followed by the Tukey pairwise comparison was performed for comparison of haemodynamic parameters among groups. 95% confidence intervals were not adjusted for multiple comparisons; therefore, inferences drawn from them may not be reproducible.

# RESULTS

## Haemodynamic measurements

Minimal variations of flow and pressure were found among the tested configurations. **Table 1** shows the baseline haemodynamic parameters obtained from flow and pressure data across the different valve configurations. A statistically significant difference in the haemodynamic parameters was seen among all groups ($P < 0.001$). At 3 L/min, mean pressure gradients were found smaller in the MHV compared to both the THV and valve-in-MHV configurations. Similar values of PG were found at 5 L/min between MHV and THV, while the Valve-in-MHV displayed markedly higher PG. The EOA mirrored these variations, with reduced values for the valve-in-MHV at both 3 and 5 L/min.

## Flow field characteristics

The velocity field was averaged across phases including early systole, peak systole, and early diastole of the cardiac cycle (**Figure 3**). At 5 L/min, the velocities during diastole tended to zero for all cases. The systolic flow field was characterized by a central jet with a peak velocity of 1.81 m/s for the SJM MHV, 2.1 m/s for the THV, and 2.66 m/s for the Valve-in-MHV. Similarly, peak velocities at

**Table 1.** Main Haemodynamic Parameters of the Different Configurations at the Different Test Conditions

| | CO (L/min) | Flow (L/min) | Mean PG (mmHg) | EOA ($cm^2$) | RSS (Pa) | TKE ($m^2/s^2$) |
|---|---|---|---|---|---|---|
| SJM MHV | 3 | 2.98±0.02 | 5.42±0.2 | 1.41±0.17 | 105±2.3 | 0.19±0.02 |
| | 5 | 5.05±0.02 | 11.5±0.4 | 1.78±0.08 | 120±3.5 | 0.26±0.03 |
| CoreValve THV | 3 | 3.01±0.01 | 7.55±0.4 | 1.36±0.1 | 114±1.9 | 0.24±0.03 |
| | 5 | 4.96±0.02 | 10.89±0.29 | 1.88±0.12 | 261±4.2 | 0.31±0.04 |
| Valve-in-MHV | 3 | 3.10±0.01 | 10.01±0.3 | 1.18±0.09 | 245±4.4 | 0.47±0.05 |
| | 5 | 5.1±0.01 | 15.53±0.48 | 1.44±0.08 | 377±6.3 | 0.53±0.07 |

Abbreviations: CO, cardiac output; EOA, effective orifice area; PG, pressure gradient; RSS, Reynolds shear stress; SJM MHV, St Jude medical mechanical heart valve; TKE, turbulent kinetic energy; THV, turbulent kinetic energy.

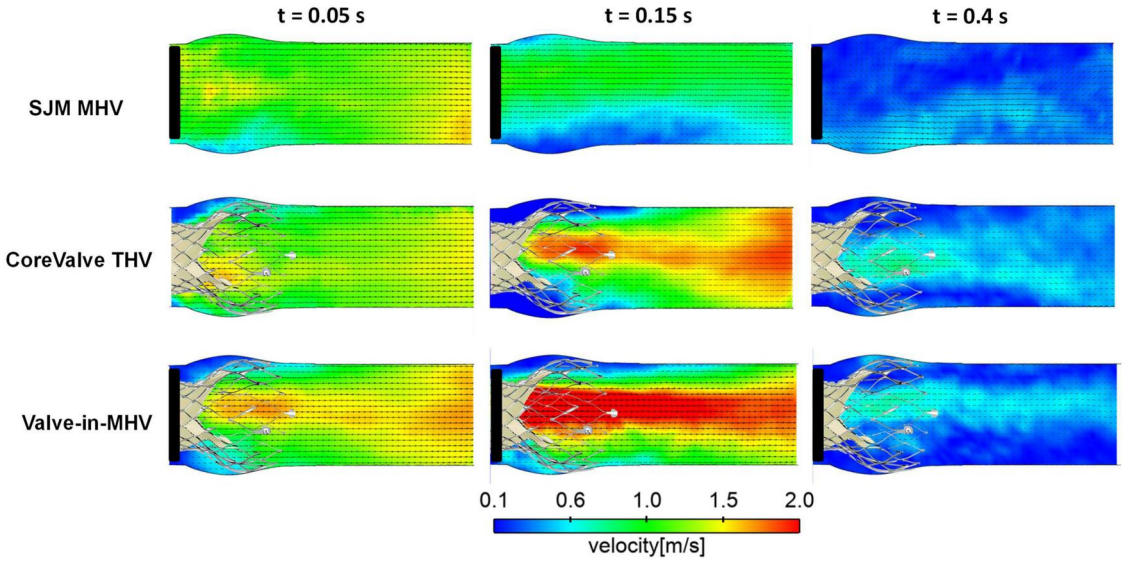


**Figure 3.** Phase-Averaged Velocity Field Past the SJM MHV, THV, and Valve-in-MHV at 5 L/min at t = 0.05 s, t = 0.15 s, and t = 0.4

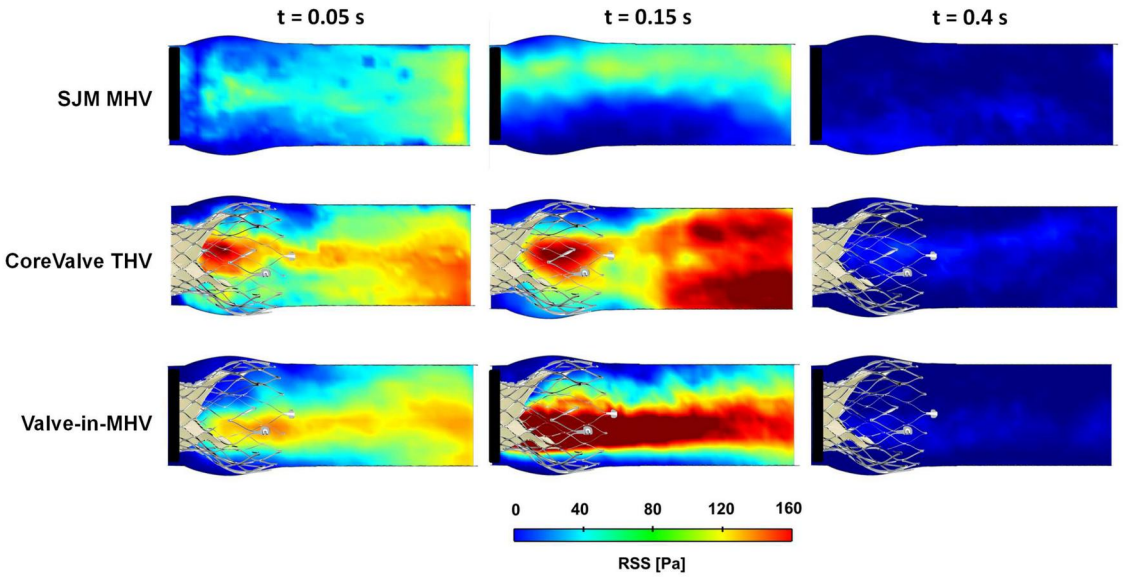


**Figure 4.** RSS Contours for the SJM MHV, THV, and Valve-in-MHV at 5 L/min at t = 0.05 s, t = 0.15 s, and t = 0.4

3 L/min were 1.09 m/s for the SJM MHV, 1.35 m/s for the THV, and 1.74 m/s for the Valve-in-MHV.

**Figure 4** displays the RSS distribution during transvalvular flow phases, with contours that correspond to the velocity fields. A consistent increase in the magnitude of both RSS and TKE values was observed from the SJM MHV, through the THV, to the Valve-in-MHV configuration at both 3 and 5 L/min. The THV and Valve-in-MHV configurations experience higher RSS and TKE magnitude than the MHV. At 5 L/min, the THV and the Valve-in-MHV exhibited, respectively, peak RSS of 261 and 377 Pa and TKE of 0.31 and 0.53 $m^2/s^2$. While for the MHV the peak RSS and TKE values were calculated to be, respectively, 120 Pa and 0.26 $m^2/s^2$. High TKE values propagated conically in the x-direction for the THV and Valve-in-MHV configurations, peaking near the valve opening and becoming more homogeneous further downstream of the valve. In contrast, the SJM MHV had a skewed flow jet impinging on the onside of the vessel wall and shows a dispersed distribution with the lowest magnitudes of both RSS and TKE.

## DISCUSSION

This study aimed to assess the haemodynamic performance of Valve-in-MHV as simulated by surgically inserting the CoreValve THV into a SJM MHV composite graft, following leaflets removal. This concept arises from complex clinical scenarios in which mechanical composite grafts fail, and conventional redo surgery may be associated with prohibitive risk, or where management of anticoagulation-related complications is a major concern. In such cases, a less invasive strategy that avoids full root replacement—while potentially limiting the mechanical components contributing to thrombogenicity—could offer an alternative approach. To the best of our knowledge, this is the first study to

present experimental results on such a hybrid configuration. The haemodynamics of the Valve-in-MHV configuration was evaluated using PIV in a mock circulatory loop and compared to those of the SJM MHV and the THV alone. Despite minor differences in mean flow rate and pressure, the similar testing conditions allowed for both qualitative and quantitative comparisons.

Agreement was found in the pressure gradient and EOA estimations at physiological condition of 5 L/min for the SJM MHV and THV in Hatoum et al.[20] For all the valves, the increase of the transvalvular pressure gradient correlated with the increase of the CO. Additionally, an inverse relationship was observed between PG and the EOA. Overall, the Valve-in-MHV configuration demonstrated the highest PG and the smallest EOA at both CO levels of 3 and 5 L/min. In contrast, the SJM MHV exhibited a significant variation in PG and EOA values between the 2 CO conditions, indicating greater sensitivity to changes in flow rate. Although the SJM MHV presented better pressure gradients at 3 L/min, the THV was found to have the best haemodynamic performance in terms of pressure gradient at 5 L/min, despite having a slightly smaller EOA compared to the other valves.

The biological valve generated a prominent central flow jet in both the THV and Valve-in-MHV configurations. The distributions of RSS and TKE followed similar patterns to the velocity field, exhibiting higher magnitudes in the Valve-in-MHV configuration compared to the THV configuration and SJM MHV.

Both simulated COs led to similar haemodynamic patterns, with lower magnitudes of the investigated parameters for the low flow rate of 3 L/min. Although the flow dynamics of the Valve-in-MHV configuration demonstrated a physiological flow pattern, the increased predisposition towards high velocities due to further constriction of the aortic annulus raises concerns regarding potential adverse effects. While this technique does not inherently eliminate the need for anticoagulation, its potential to simplify reintervention and reduce metallic leaflet-related thrombogenicity could have clinical utility in selected high-risk patients. Indeed, the increased pressure gradient, decreased EOA and turbulent flow can increase the likelihood of thrombotic events in the hybrid configuration, as increased turbulence corresponds to excessive stress on platelets and their activation.[15,21] However, this may be less harmful with greater diameters of the original MHV conduit. In addition to radial constraint, a mismatch in valves' height may also negatively influence Valve-in-MHV haemodynamics. Specifically, partially overhanging leaflets are discouraged, as they have been associated with increased regurgitation and disruption of central flow.[22]

The most striking finding was the increase in flow velocity and turbulence parameters in the Valve-in-MHV configuration. We speculate that the disturbed flow in the Valve-in-MHV configuration resulted from the limited expansion of the THV within the stiff metallic ring of the MHV. This is consistent with the actual inner diameters, ie, 19.5 mm for the MHV and 23 mm for the THV. This hypothesis is further supported by the elevated pressure gradient and small EOA values observed in the Valve-in-MHV experiments, which correlated with increased TKE levels, being 1.5-fold higher than the TAVI scenario. Future investigations should evaluate the effect of THV sizing on flow characteristics in Valve-in-MHV procedures, including whether a smaller diameter (e.g., 23 mm) could achieve improved haemodynamic outcomes.

Our results are consistent with those of Hatoum et al[20,23] who documented turbulent wakes of varying intensities impinging on the aortic walls, reporting peaks of TKE and RSS for the THV. These studies indicated that the shear stress of THVs can exceed the 10-100 Pa range during peak systole, which has been reported to induce blood damage and thrombus formation.[15] After valve-in-valve (ViV) procedures, the shear stress further increases 2- to 3-fold to cause thrombus formation and haemolysis.[24,25] In this study, we observed an increase in flow velocity and turbulence parameters in the Valve-in-MHV configuration, underscoring the effect of the ViV procedure on the resulting haemodynamics.

From a clinical perspective, this emphasizes the critical need for further research into procedure optimization to mitigate adverse haemodynamic effects and improve patient outcomes.

Despite the increasing use of the ViV procedure, *in vitro* investigations on the haemodynamics of ViV procedures are still relatively sparse.[23] Overall, these investigations have highlighted that post-ViV haemodynamics vary according to different device types, sizes and implantation depths, particularly in terms of the effect on sinus washout. However, the present study extends beyond the existing research by examining the haemodynamic performance of a novel hybrid approach by simulating the insertion of the THV into a composite valved graft. Breaking the carbon leaflets before implanting a THV into the remaining ring was described by Butter et al.[26] They reported the first-in-human successful implantation of a balloon-expandable THV within the remaining ring of a mechanical valve via a fully percutaneous procedure. Nonetheless, anticoagulant therapy was still deemed necessary due to the presence of metallic fragments post-leaflet breakage. We found increased flow velocity and turbulence in the Valve-in-MHV configuration, suggesting that anticoagulation should be maintained not only due to metallic fragments but also because of the altered haemodynamics. However, this does not imply that Valve-in-MHV is unfeasible, as a larger metallic ring may provide a better expansion of the THV. Therefore, careful patient selection is suggested for Valve-in-MHV application.

## Limitations

This study used a 3 D-printed annulus ring to replicate the SJM mechanical valve, instead of a full mechanical Bentall graft. A thick-walled silicone phantom with similar circumferential properties was used to simulate the Dacron graft. While this substitution may not fully capture the mechanical behaviour of a real composite graft, it enabled reproducible, optically accessible testing of the valve-in-MHV configuration under controlled conditions.

As no primary end-point was prespecified and no adjustment for multiple testing was performed, the reported statistical results should be interpreted as exploratory.

Factors such as implantation depth, device size, and typology were not investigated. It is likely that the disadvantageous effects measured in the THV in a 21 mm SJM prosthesis will be mitigated in larger annuli (e.g., 23- or 25-mm valves). Moreover, clinical protocols often recommend using balloon-expandable valves in very small surgical valves to minimize transvalvular gradients. Although coronary flow assessment is an important component in ViV procedures, it was not included in this study to primarily focus mostly on the valve's flow dynamics.

The backlight PIV setup inherently restricts the measurement to a 2dimensional plane, which may not fully capture the complex 3D flow dynamics. Furthermore, the use of a backlight may contaminate flow information in the central jet due to particles

close to the walls of the phantom in front or behind the mid-plane. Although the small depth of field of the PIV camera mitigates this effect, it could result in less accurate representation of flow patterns, particularly in areas critical to thrombus formation. Future studies could employ tomographic PIV to provide 3D flow data, offering a more comprehensive understanding of flow dynamics.

## CONCLUSION

Results shed light on the haemodynamic performance of Valve-in-MHV interventions involving the surgical implantation of the THV within a composite valved graft. Baseline haemodynamic parameters showed significant differences among the various implantation scenarios, with the Valve-in-MHV configuration exhibiting higher mean PG and turbulence values than the other configurations. By understanding the complex interplay between valve design and flow, clinicians can make more informed decisions to improve patient outcomes and reduce the risk of adverse events associated with hybrid ViV approaches.

## FUNDING

This work was supported by the European Commission—Next Generation EU—PNRR M6—C2—Investimento 1.3: Sviluppo di tecnologie e percorsi innovativi per la salute—Iniziativa PNC0000003 dal titolo "ANTHEM: AdvaNced Technologies for Human-centrEd Medicine"—CUP B53C22006700001.

## CONFLICTS OF INTEREST

None declared.

## DATA AVAILABILITY

There are no new data associated with this article.

## REFERENCES

[1] Leon MB, Smith CR, Mack M, PARTNER Trial Investigators, et al. Transcatheter aortic-valve implantation for aortic stenosis in patients who cannot undergo surgery. *N Engl J Med*. 2010;363:1597-1607. https://doi.org/10.1056/NEJMoa1008232
[2] Glaser N, Persson M, Jackson V, Holzmann MJ, Franco-Cereceda A, Sartipy U. Loss in life expectancy after surgical aortic valve replacement: SWEDEHEART study. *J Am Coll Cardiol*. 2019;74:26-33.
[3] Yoganathan AP, He Z, Casey Jones S. Fluid mechanics of heart valves. *Annu Rev Biomed Eng*. 2004;6:331-362.
[4] De Backer O, Wong I, Wilkins B, Carranza CL, Søndergaard L. Patient-tailored aortic valve replacement. *Front Cardiovasc Med*. 2021;8:658016.
[5] Alperi A, Garcia S, Rodes-Cabau J. Transcatheter valve-in-valve implantation in degenerated surgical aortic and mitral bioprosthesis: current state and future perspectives. *Prog Cardiovasc Dis*. 2022;72:54-65.
[6] Becsek B, Pietrasanta L, Obrist D. Turbulent systolic flow downstream of a bioprosthetic aortic valve: velocity spectra, wall shear stresses, and turbulent dissipation rates. *Front Physiol*. 2020;11:577188.
[7] Hatoum H, Girault E, Heim F, Dasi LP. *In vitro* characterization of self-expandable textile transcatheter aortic valves. *J Mech Behav Biomed Mater*. 2020;103:103559.
[8] Haya L, Tavoularis S. Comparison of *in vitro* flows past a mechanical heart valve in anatomical and axisymmetric aorta models. *Exp Fluids*. 2017;58:73.
[9] Girardi LN, Talwalkar NG, Coselli JS. Aortic root replacement: results using the St Jude Medical/hemashield composite graft. *Ann Thorac Surg*. 1997;64:1032-1035.
[10] Jahren SE, Winkler BM, Heinisch PP, Wirz J, Carrel T, Obrist D. Aortic root stiffness affects the kinematics of bioprosthetic aortic valves. *Interact CardioVasc Thorac Surg*. 2017;24:173-180.
[11] De Paulis R, Scaffa R, Weltert L, Salica A. Mimicking mother nature: the valsalva graft. *J Thorac Cardiovasc Surg*. 2020;159:1758-1763.
[12] Ferrari G, Balasubramanian P, Tubaldi E, Giovanniello F, Amabili M. Experiments on dynamic behaviour of a Dacron aortic graft in a mock circulatory loop. *J Biomech*. 2019;86:132-140.
[13] Hasler D, Obrist D. Three-dimensional flow structures past a bioprosthetic valve in an *in vitro* model of the aortic root. *PLoS One*. 2018;13:e0194384.
[14] Stamhuis E, Thielicke W. PIVlab—towards user-friendly, affordable and accurate digital particle image velocimetry in MATLAB. *J Open Res Softw*. 2014;2:30.
[15] Dasi LP, Hatoum H, Kheradvar A, et al. On the mechanics of transcatheter aortic valve replacement. *Ann Biomed Eng*. 2017;45:310-331.
[16] Ferrari L, Obrist D. Comparison of hemodynamic performance, three-dimensional flow fields, and turbulence levels for three different heart valves at three different hemodynamic conditions. *Ann Biomed Eng*. 2024;52:3196-3207.
[17] Pope SB. Turbulent flows. *Meas Sci Technol*. 2001;12:2020-2021.
[18] Giersiepen M, Wurzinger L, Opitz R, Reul H. Estimation of shear stress-related blood damage in heart valve prostheses-*in vitro* comparison of 25 aortic valves. *Int J Artif Organs*. 1990;13:300-306.
[19] Morbiducci U, Ponzini R, Nobili M, et al. Blood damage safety of prosthetic heart valves. Shear-induced platelet activation and local flow dynamics: a fluid–structure interaction approach. *J Biomech*. 2009;42:1952-1960.
[20] Hatoum H, Ahn S, Lilly S, et al. Flow dynamics of surgical and transcatheter aortic valves: past to present. *JTCVS Open*. 2022;9:43-56.
[21] Hathcock JJ. Flow effects on coagulation and thrombosis. *Arterioscler Thromb Vasc Biol*. 2006;26:1729-1737.
[22] Chen H, Samaee M, Yadav P, Thourani V, Dasi LP. Effects of implantation height on the performance of a redo transcatheter aortic valve replacement using a balloon-expandable valve. *JTCVS Open*. 2024;19:61-67.
[23] Hatoum H, Lilly S, Maureira P, Crestanello J, Dasi LP. The hemodynamics of transcatheter aortic valves in transcatheter aortic valves. *J Thorac Cardiovasc Surg*. 2021;161:565-576 e2. https://doi.org/10.1016/j.jtcvs.2019.09.174
[24] Rosseel L, De Backer O, Søndergaard L. Clinical valve thrombosis and subclinical leaflet thrombosis following transcatheter aortic valve replacement: is there a need for a patient-tailored antithrombotic therapy? *Front Cardiovasc Med*. 2019;6:44.
[25] Marwan M, Mekkhala N, Göller M, et al. Leaflet thrombosis following transcatheter aortic valve implantation. *J Cardiovasc Comput Tomogr*. 2018;12:8-13.
[26] Butter C, Kühnel R-U, Hölschermann F. First successful transcatheter valve-in-valve implantation into a failed mechanical prosthetic aortic valve facilitated by fracturing of the leaflets: a case report. *Eur Heart J Case Rep*. 2021;5:ytab130.


Interdisciplinary CardioVascular and Thoracic Surgery, 2025, 40, ivaf265
https://doi.org/10.1093/icvts/ivaf265
Original article